Vehicular Communications 19 (2019) 100166

Contents lists available at ScienceDirect

Vehicular Communications

www.elsevier.com/locate/vehcom

Performance analysis of vehicle-to-vehicle communication with full-duplex amplify-and-forward relay over double-Rayleigh fading channels

Ba Cao Nguyen [a], Tran Manh Hoang [a], Le The Dung [b,c,*,1]

[a] Faculty of Radio Electronics, Le Quy Don Technical University, Viet Nam
[b] Division of Computational Physics, Institute for Computational Science, Ton Duc Thang University, Ho Chi Minh City, Viet Nam
[c] Faculty of Electrical and Electronics Engineering, Ton Duc Thang University, Ho Chi Minh City, Viet Nam

ARTICLE INFO

Article history:
Received 1 March 2019
Received in revised form 17 June 2019
Accepted 3 July 2019
Available online 16 July 2019

Keywords:
Vehicle-to-vehicle communication
Full-duplex
Self-interference cancellation
Amplify-and-forward
Outage probability
Symbol error rate

ABSTRACT

In this paper, we investigate a vehicle-to-vehicle (V2V) communication system where a full-duplex (FD) relay uses amplify-and-forward (AF) protocol. We consider two cases of the AF protocol at the FD relay, i.e. fixed and variable gain relaying. Furthermore, the channels between the nodes are characterized as the double (cascaded) Rayleigh fading distributions. We derive the exact closed-form expressions of the outage probabilities (OPs) and symbol error rates (SERs) in these two cases. Numerical results show the impacts of the double Rayleigh fading channels on the system performance in comparison with those of Rayleigh fading channels. Moreover, the effects of the distance, path loss exponent, and residual self-interference (RSI) on the system performance are also studied. We find that for a given node transmission power, there exist optimal distances between vehicles for the fixed and variable gain relaying which provide the best system performance. All analysis results in this paper are validated by Monte-Carlo simulation results to confirm the correctness of the derived mathematical expressions.

1. Introduction

In the age of digital technology, almost personal devices are connected to the Internet to exchange data. Not only support voice and video communications, smart devices are also linked with other devices to perform many operations such as in smart home, intelligent transportation systems (ITS). Recently, device-to-device (D2D) communication is fast developed, leading to the demand of big data for the Internet of Things (IoT) and the fifth generation (5G) of mobile communications. To solve the problem of limited spectrum in wireless networks, various methods have been proposed such as massive multiple-input multiple-output (MIMO), full-duplex (FD), non-orthogonal multiple access (NOMA) [1–3].

Among these methods, FD communication has become a hot topic due to the fact that FD devices can transmit and receive the signal at the same time and on the same frequency band, that leads to the capability of doubling the system capacity. With the development of antenna design techniques and the analog and digital signal processing, FD devices can suppress the self-interference cancellation (SIC) up to 110 dB in both theories and practices [4,5]. Therefore, FD communication is a promising solution for the future wireless networks and the research on FD system has been conducted in many aspects such as the SIC techniques [5–7], the performance analysis in terms of the outage probability (OP), and the ergodic capacity [3,8–11].

In the literature, due to the benefits of using relay node in wireless systems, such as enhancing the reliability, coverage, and the performance of wireless systems [12,13], many works have analyzed the relay systems where the FD relay is used to improve the spectral efficiency [3,8,10,14,15]. Their results showed that the system with FD relay can be applied in the realistic scenarios where various SIC are conducted to alleviate the self-interference. In these studies, the OP, symbol error rate (SER), and the ergodic capacity were analyzed in the case of imperfect SIC at FD relay node. The authors demonstrated that the FD systems can nearly double the spectrum when the RSI is very small. Additionally, the OP and SER of these systems reached the error floor due to the RSI. In [9,15], optimal power allocation schemes for the FD mode were proposed to reduce the impact of the RSI and improve the system performance.

* Corresponding author at: 19 Nguyen Huu Tho street, Tan Phong ward, District 7, Ho Chi Minh City, Viet Nam.
E-mail addresses: bacao.sqtt@gmail.com (B.C. Nguyen), tranmanhhoang@tcu.edu.vn (T.M. Hoang), lethedung@tdtu.edu.vn (L.T. Dung).
[1] Member IEEE.

https://doi.org/10.1016/j.vehcom.2019.100166
2214-2096/

Today, vehicular communications play an important role due to their applications in autonomous vehicles [16–20]. Moreover, almost people control the system through the smart devices even when these devices move on the road, which form the vehicle-to-vehicle (V2V) communication. Since the channels between the devices in V2V communication exhibit double Rayleigh fading, they are worse than the channels in traditional wireless communication where the channels between the devices are usually characterized by Rayleigh fading. Therefore, the system performance of V2V communication will be decreased in comparison with that of traditional wireless communication. Due to the fact that the V2V communication can be applied for the intelligent transportation systems (ITS) [19,20], it is vitally necessary to analyze and improve the system performance. As a result, a lot of researches have focused on the applications, architectures, protocols, and channel models of V2V communications.

Particularly, in V2V communication systems, since all nodes are vehicles, the random distributions such as Rayleigh, Rician, or Nakagami-*m* which are often used to model the fading of traditional wireless channels do not fit for almost V2V channels [21–23]. It is because those channels are often applied for stationary communication links, where all nodes are fixed. In contrast, the theoretical analysis and field measurement [21–23] demonstrated that the double Rayleigh fading distribution can precisely characterize the V2V channel, because the two-bounce scattering components caused by the scatterers in the surrounding transmitter's and receiver's local environment will generate cascaded (double) Rayleigh fading distributions [22]. Furthermore, the double Rayleigh fading distribution also fits for various scenarios such as suburban outdoor-to-indoor mobile-to-mobile communication scenarios or keyhole channels [24].

The effects of double Rayleigh fading channels on the V2V communication systems have been analyzed in several works in the literature [18,20,25–28]. Their results showed that the double Rayleigh fading channels greatly reduce the system performance strongly in both theoretical analysis and experiments. The system performance of point-to-point HD-V2V communication over double Rayleigh fading channels was analyzed in [20,29]. Recently, the combination of the FD technique with V2V communication in a system has been conducted, such as in [19,30–32]. The work in [19] discussed the advantages and disadvantages of the FD-V2V communication. In addition, the guideline for the design and the deployment of medium access control was also given. The authors of [30] showed that a FD vehicle can detect collision and apply this ability in cooperative automated driving. Realizing the importance of antenna design to the FD-V2V communication, [31] proposed a novel dual-band full-duplex antenna array. In this antenna array, the authors used two ports to increase the isolation between the transmitted signal and received signal, resulting in a decreased self-interference. Furthermore, the size, weight, and cost of this antenna array was reduced because the filtering, duplexing, and radiation were combined into a single device. In [32], the FD vehicular access networks without the channel state information (CSI) at the transmitter was investigated. The optimal blind interference alignment scheme was proposed to improve the sum rate of the system.

We observe that there is a lack of research on FD-V2V communication systems. It is because when FD and V2V communication are combined, the system performance will be decreased due to the impacts of the RSI in FD mode and the double Rayleigh fading channels. Furthermore, the channels in V2V communication are considered as double Rayleigh fading channels which increases the computation complexity. Therefore, all previous works did not derive mathematical expressions of OP and SER. Motivated by this issue, in this paper, we propose the novel model which combines the FD and V2V communication into a system. In this system, source node which operates in half-duplex (HD) mode transmits signal to destination node via relay node which operates in FD mode. The relay node uses amplify-and-forward (AF) protocol with fixed and variable gain relaying.

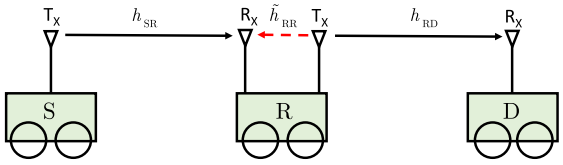

Fig. 1. System model of the V2V communication system with FD relay. (For interpretation of the colors in the figure(s), the reader is referred to the web version of this article.)

The contributions of this paper can be summarized as follows:

– We consider the FD relay system where all nodes are vehicles and perform FD-V2V communications. At the FD relay node, we investigate two cases of AF protocol, i.e. fixed and variable gain relaying with imperfect SIC. The channels between nodes are considered as double Rayleigh fading channels.

– We successfully derive the exact closed-form expressions of the OP and SER in the case of imperfect SIC at the FD relay node for fixed and variable gain relaying. Based on these expressions, the system throughput is also studied.

– We show that for both cases fixed and variable gain relaying, the performance of the considered FD-V2V communication system strongly degrades compared with the performance of that system over Rayleigh fading channels. In addition, the system performance is significantly affected by the RSI due to the FD mode. The impacts of the distance between vehicles and the path loss exponent are also investigated. We observe that there exist different optimal distances between vehicles which provides the best system performance for fixed and variable gain relaying. Finally, the Monte-Carlo simulations are used to validate the analysis results.

The rest of this paper is organized as follows. Section 2 describes the signal and system models, while Section 3 presents the analysis of system performance in terms of the OP and SER. Section 4 gives the numerical results and discussions. Finally, Section 5 concludes the paper.

2. System model

In this section, the signal and system models of a FD-V2V communication system is described. As illustrated in Fig. 1, the signal is transmitted from a source node (S) to a destination node (D) via a relay node (R). In this system, R operates in FD mode with two antennas, one for transmitting and the other for receiving. Meanwhile, S and D operate in the HD mode with single antenna. We should note that in practical system, R can use one shared-antenna for both transmitting and receiving by using a circulator to separate the transmitted and received signals. However, when using two separate antennas various SIC techniques such as the isolation, the analog and digital cancellations can be easily applied to FD relay [4,33]. Therefore, in this paper, we assume that the relay uses two separate antennas to obtain good SIC capability.

On the other hand, the relay uses AF protocol. We investigate two cases of AF protocol at the relay node. Specifically, when the relay node knows the instantaneous channel gain from the source node to the relay node, it uses variable-gain relaying. Otherwise, it uses fixed-gain relaying. Furthermore, all nodes are mobile vehicles which form a V2V communication system. Therefore, the source-relay and relay-destination channels are considered as independent and identically distributed (IID) double Rayleigh random variables (RVs).

At the time slot t, R receives signal from S. This received signal can be expressed as

$$y_R = \sqrt{d_{SR}^{-\alpha} P_S} h_{SR} x_S + \tilde{h}_{RR} \sqrt{d_{RR}^{-\alpha} P_R} x_R + n_R, \quad (1)$$

where d_{SR} and d_{RR} are the distances between S and R and between the transmission antenna and reception antenna of R, respectively; α is the path loss exponent and its value ranges from 2 to 6; h_{SR} and $\tilde{h}_{RR}$ are respectively the fading coefficients of the channels from S to R and from the transmitting to the receiving antennas of R; x_S and x_R represent the complex signals which are transmitted from S and R, respectively; n_R is the Additive White Gaussian Noise (AWGN) with zero-mean and variance of σ^2, i.e. $n_R \sim \mathcal{CN}(0, \sigma^2)$. It is also noted that, in the literature such as [34], the interference between vehicles can be utilized in various applications such as energy harvesting, channel estimation, message flooding, link security and signal alignment. However, in this scenario the SI signal is not a useful signal and the relay must suppress it to improve the system performance.

As aforementioned, the relay node can combine all SIC techniques [5,6,33,35]. However, due to the imperfect SIC, the residual self-interference (RSI) still strongly impacts the system performance. Specifically, after applying all SIC techniques, the RSI, denoted by I_R, can be modeled as the Gaussian distribution [5,6, 33] with zero mean and variance of γ_{RSI}, which is well-fitted with the measurement and experiment results [4,8–10]. On the other hand, this assumption helps us reduce the number of variables in mathematical expressions because when we consider I_R as a Gaussian variable, its variance is a constant. It is noted that $\gamma_{RSI} = \tilde{\Omega} P_R$, where $\tilde{\Omega}$ refers to the SIC capability of the FD node. Therefore, the received signal at R after SIC can be rewritten as

$$y_R = \sqrt{d_{SR}^{-\alpha} P_S} h_{SR} x_S + I_R + n_R. \quad (2)$$

Due to the AF protocol, the transmitted signal at the R is its previous received signal after amplifying, that means $x_R = G y_R$, where G is the relaying gain which is subjected to the normalized transmission power of the relay. Furthermore, because of the double Rayleigh channels, h_{SR} is the multiplication of two independent Rayleigh variables g_1 and g_2, i.e. $h_{SR} = g_1 g_2$. Therefore, the fixed gain (G_f) and the variable gain (G_v) corresponding to the channel conditions are calculated as

$$G_f \triangleq \sqrt{\frac{1}{d_{SR}^{-\alpha} \Omega_1 \Omega_2 P_S + \gamma_{RSI} + \sigma^2}}, \quad (3)$$

$$G_v \triangleq \sqrt{\frac{1}{d_{SR}^{-\alpha} \rho_1 \rho_2 P_S + \gamma_{RSI} + \sigma^2}}, \quad (4)$$

where $\rho_1 = |g_1|^2$ and $\rho_2 = |g_2|^2$ are the instantaneous channel gains, $\Omega_1 = \mathbb{E}\{\rho_1\}$, $\Omega_2 = \mathbb{E}\{\rho_2\}$, $\mathbb{E}\{\cdot\}$ denotes the expectation operator.

According to the FD mode, the relay forwards the signal to the destination after amplifying this signal at the same time and on the same frequency band. Therefore, the received signal at D is given by

$$y_D = \sqrt{d_{RD}^{-\alpha} P_R} h_{RD} x_R + n_D, \quad (5)$$

where d_{RD} is the distance between R and D; h_{RD} is the fading coefficient of R–D link; n_D is the AWGN at the destination D, $n_D \sim \mathcal{CN}(0, \sigma^2)$. It is also noted that h_{RD} has the same distribution with h_{SR}, that means $h_{RD} = g_3 g_4$, where g_3 and g_4 are two independent Rayleigh variables. Substituting x_R by $G y_R$, we have

$$y_D = \sqrt{d_{RD}^{-\alpha} P_R} h_{RD} G \left(\sqrt{d_{SR}^{-\alpha} P_S} h_{SR} x_S + I_R + n_R \right) + n_D. \quad (6)$$

From (6), the end-to-end signal-to-interference-plus-noise ratios (SINRs) for the cases of fixed and variable gain relaying are respectively computed as

$$\gamma_f = \frac{(d_{SR} d_{RD})^{-\alpha} P_S P_R |h_{SR}|^2 |h_{RD}|^2}{d_{RD}^{-\alpha} P_R |h_{RD}|^2 (\gamma_{RSI} + \sigma^2) + \sigma^2 / G_f^2} = \frac{(d_{SR} d_{RD})^{-\alpha} P_S P_R \rho_1 \rho_2 \rho_3 \rho_4}{d_{RD}^{-\alpha} P_R \rho_3 \rho_4 (\gamma_{RSI} + \sigma^2) + \sigma^2 / G_f^2}, \quad (7)$$

$$\gamma_v = \frac{(d_{SR} d_{RD})^{-\alpha} P_S P_R \rho_1 \rho_2 \rho_3 \rho_4}{d_{RD}^{-\alpha} P_R \rho_3 \rho_4 (\gamma_{RSI} + \sigma^2) + \sigma^2 (d_{SR}^{-\alpha} P_S \rho_1 \rho_2 + \gamma_{RSI} + \sigma^2)}, \quad (8)$$

where $\rho_3 = |g_3|^2$ and $\rho_4 = |g_4|^2$.

3. System performance

3.1. Outage probability

The OP of the considered system is defined as the probability that the transmission rate of the system is less than a given data rate. We assume that the minimum required data rate of the system is $\mathcal{R}$ (bit/s/Hz), thus the OP is calculated as

$$P_{out} = \Pr\{\log_2(1+\gamma) < \mathcal{R}\} = \Pr\{\gamma < 2^{\mathcal{R}} - 1\}, \quad (9)$$

where γ is the SINR which is determined by (7) for the case of fixed gain relaying and by (8) for the case of variable gain relaying. Let $\gamma_0 = 2^{\mathcal{R}} - 1$ be the threshold of the OP, then (9) becomes

$$P_{out} = \Pr\{\gamma < \gamma_0\}. \quad (10)$$

Theorem 1. *The* OPs *of the FD relay system over double Rayleigh fading channels and under the impact of the RSI in the cases of fixed gain* (P_{out}^f) *and variable gain* (P_{out}^v) *are expressed as follows*

$$P_{out}^f = 1 - \frac{\pi C_f}{2M} \sum_{m=1}^{M} \frac{\sqrt{1-\phi_m^2}}{z} \sqrt{\frac{A_f \gamma_0}{-\ln z} + B_f \gamma_0} \times K_0\left(\sqrt{-2C_f \ln z}\right) K_1\left(\sqrt{\frac{A_f \gamma_0}{-\ln z} + B_f \gamma_0}\right), \quad (11)$$

$$P_{out}^v = 1 - \frac{\pi C_v}{2M} \sum_{m=1}^{M} \frac{\sqrt{1-\phi_m^2}}{z} \sqrt{\frac{A_v(\gamma_0^2 + \gamma_0)}{-\ln z} + B_v \gamma_0} \times K_0\left(\sqrt{-2C_v \ln z + D_v \gamma_0}\right) K_1\left(\sqrt{\frac{A_v(\gamma_0^2 + \gamma_0)}{-\ln z} + B_v \gamma_0}\right), \quad (12)$$

where

$$A_f = \frac{4\sigma^2}{(d_{SR} d_{RD})^{-\alpha} \Omega_1 \Omega_2 P_S P_R G_f^2}; \; B_f = \frac{4(\gamma_{RSI} + \sigma^2)}{d_{SR}^{-\alpha} \Omega_1 \Omega_2 P_S};$$

$$C_f = \frac{2}{\Omega_3 \Omega_4}; \; A_v = \frac{4\sigma^2(\gamma_{RSI} + \sigma^2)}{(d_{SR} d_{RD})^{-\alpha} \Omega_1 \Omega_2 P_S P_R};$$

$$B_v = B_f; \; C_v = C_f; \; D_v = \frac{4\sigma^2}{d_{RD}^{-\alpha} \Omega_3 \Omega_4 P_R}$$

$$z = \frac{1}{2} + \frac{1}{2}\phi_m; \; \phi_m = \cos\left(\frac{(2m-1)\pi}{2M}\right);$$

$\Omega_i = \mathbb{E}\{\rho_i\}$ is the average channel gain of link i, $i = 1, 2, 3, 4$; M is the complexity-accuracy trade-off parameter; $K_0(.)$ and $K_1(.)$ denote the zero and the first-order modified Bessel functions of the second kind, respectively.

Proof. The detailed proof is presented in Appendix A. □

3.2. Symbol error rate

The SER of the wireless system is given by [36]

$$\text{SER} = a\mathbb{E}\left\{Q\left(\sqrt{b\gamma}\right)\right\} = \frac{a}{\sqrt{2\pi}}\int_0^{\infty} F\left(\frac{u^2}{b}\right)e^{-\frac{u^2}{2}}du, \tag{13}$$

where a and b are constants and their values depend on the modulation types [36], e.g. $a = 2, b = 1$ for quadrature phase shift keying (QPSK) and 4-quadrature amplitude modulation (4-QAM), $a = 1, b = 2$ for the binary phase-shift keying (BPSK) modulation; $Q(x) = \frac{1}{\sqrt{2\pi}}\int_x^{\infty} e^{-u^2/2}du$ is the Gaussian function; γ and $F(.)$ are respectively the end-to-end SINR and its CDF. It is noted that from the definition of the CDF and the OP, we can replace $F(x)$ by the P_{out} of the system which are specified in (11) and (12).

Theorem 2. *The* SER*s in the cases of fixed gain relaying* (SER_{f}) *and variable gain relaying* (SER_{v}) *of the system are obtained as follows*

$$\begin{aligned}\text{SER}_{\text{f}} = \frac{a\sqrt{b}}{2\sqrt{2\pi}}\Bigg[&\sqrt{\frac{2\pi}{b}} - \frac{\pi C_{\text{f}}}{2M}\sum_{m=1}^{M}\frac{\sqrt{1-\phi_m^2}}{z}\sqrt{\frac{A_{\text{f}}}{-\ln z}+B_{\text{f}}}\\ &\times K_0\left(\sqrt{-2C_{\text{f}}\ln z}\right)\exp\left(\frac{1}{4b}\left(\frac{A_{\text{f}}}{-\ln z}+B_{\text{f}}\right)\right)\\ &\times\frac{\Gamma\left(\frac{3}{2}\right)\Gamma\left(\frac{1}{2}\right)}{\sqrt{\frac{b}{2}\left(\frac{A_{\text{f}}}{-\ln z}+B_{\text{f}}\right)}}W_{-\frac{1}{2},\frac{1}{2}}\left(\frac{1}{2b}\left(\frac{A_{\text{f}}}{-\ln z}+B_{\text{f}}\right)\right)\Bigg],\end{aligned} \tag{14}$$

$$\begin{aligned}\text{SER}_{\text{v}} = \frac{a\sqrt{b}}{2\sqrt{2\pi}}\Bigg[&\sqrt{\frac{2\pi}{b}} - \frac{\pi^2 C_{\text{v}}}{2bMN}\sum_{m=1}^{M}\sum_{n=1}^{N}\frac{\sqrt{1-\phi_m^2}}{z}\\ &\times\sqrt{1-\phi_n^2}\sqrt{\frac{A_{\text{v}}(b-2\ln t)}{-b\ln z}+B_{\text{v}}}\\ &\times K_0\left(\sqrt{-2C_{\text{v}}\ln z-\frac{2D_{\text{v}}\ln t}{b}}\right)\\ &\times K_1\left(\sqrt{-\frac{2}{b}\left[\frac{A_{\text{v}}(b-2\ln t)}{-b\ln z}+B_{\text{v}}\right]\ln t}\right)\Bigg],\end{aligned} \tag{15}$$

where Γ *and* W *are respectively the Gamma and Whittaker functions [37];* N *is the complexity-accuracy trade-off parameter;* $t = \frac{1}{2} + \frac{1}{2}\phi_n$; $\phi_n = \cos\left(\frac{(2n-1)\pi}{2N}\right)$.

Proof. The detailed proof is presented in Appendix B. □

4. Numerical results and discussion

In this section, we evaluate the system performance by using the mathematical expressions in Theorems 1 and 2. Furthermore, we also use the Monte-Carlo simulations and plot both the theory and simulation curves on a figure to demonstrate the correctness of the derived mathematical expressions. It is noted that the SNR in this paper is the ratio of the transmission power (P_{S} and P_{R}) to the variance of AWGN (σ^2), i.e. $\text{SNR} = P_{\text{S}}/\sigma^2 = P_{\text{R}}/\sigma^2$. The average channel gains $\Omega_i = 1$ with $i \in \{1, 2, 3, 4\}$. The SIC capability $\tilde{\Omega}$ is varied to evaluate the impact of the RSI on the system performance. The distance d_{SR} and d_{RD} are chosen so that $d_{\text{SR}} + d_{\text{RD}} = 1$, which is similar to [28,38].

Fig. 2 investigates the OPs of the considered FD-V2V communication system versus the average SNR in the cases of fixed and variable gain relaying in comparison with this system over Rayleigh fading channels. We use $d_{\text{SR}} = d_{\text{RD}} = 0.5$ and $\alpha = 4$. The

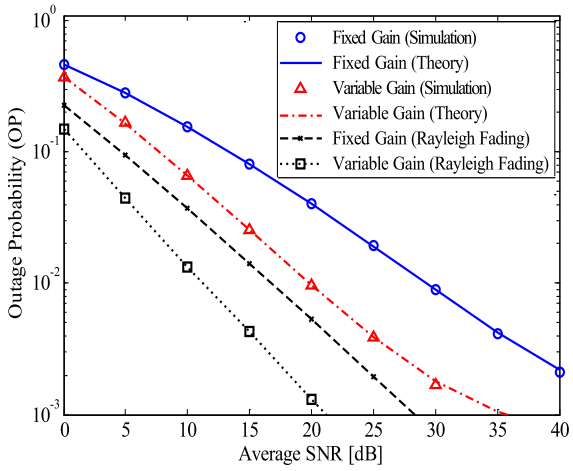

Fig. 2. The OPs of the considered FD-V2V communication system versus the average SNR in comparison with this system over Rayleigh fading channel for $\alpha = 4$, $d_{\text{SR}} = d_{\text{RD}} = 0.5$, $\tilde{\Omega} = -30$ dB, and $\mathcal{R} = 1$ bit/s/Hz.

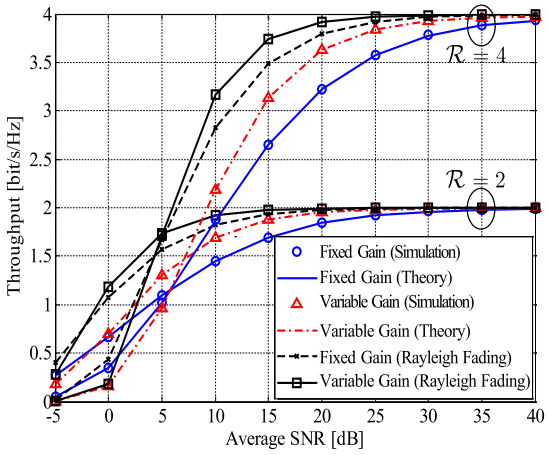

Fig. 3. The system throughput versus the average SNR, $\alpha = 4$, $d_{\text{SR}} = d_{\text{RD}} = 0.5$, $\tilde{\Omega} = -30$ dB.

minimum required data rate $\mathcal{R} = 1$ bit/s/Hz, thus the OP threshold $\gamma_0 = 2^{\mathcal{R}} - 1 = 1$. The SIC capability $\tilde{\Omega} = -30$ dB. To demonstrate the performance degradation of the system over double Rayleigh fading channels, we also conduct the simulations for this system over Rayleigh fading channel. As shown in Fig. 2, the analysis results are matched with the simulation results, confirming the correctness the mathematical expression in Theorem 1. Furthermore, the variable gain relaying increases the system performance significantly compared with the fixed-gain relaying. For example, to get $\text{OP} = 10^{-2}$, the variable gain requires approximate 5 dB and 10 dB lower SNRs for Rayleigh fading and double Rayleigh fading channels, respectively.

Fig. 3 illustrates the system throughput of the considered FD-V2V communication system with $\alpha = 4$, $d_{\text{SR}} = d_{\text{RD}} = 0.5$, $\tilde{\Omega} = -30$ dB in comparison with this system over Rayleigh fading channels. The system throughput is calculated as $\mathcal{T} = \mathcal{R}(1 - P_{\text{out}})$. In this figure, we consider two minimum required data rates, i.e. $\mathcal{R} = 2$ and $\mathcal{R} = 4$ bit/s/Hz. It is shown that in low SNR regime, the difference between the system throughput of the considered system and that of system over Rayleigh fading channel is significant. At SNR = 15 dB and $\mathcal{R} = 4$ bit/s/Hz, the system throughput of considered FD-V2V system is nearly 1 bit/s/Hz less than this system over Rayleigh fading channels. Moreover, the considered FD-V2V communication system cannot reach the required data rate, especially at high data transmission rate, i.e. $\mathcal{R} = 4$ bit/s/Hz.

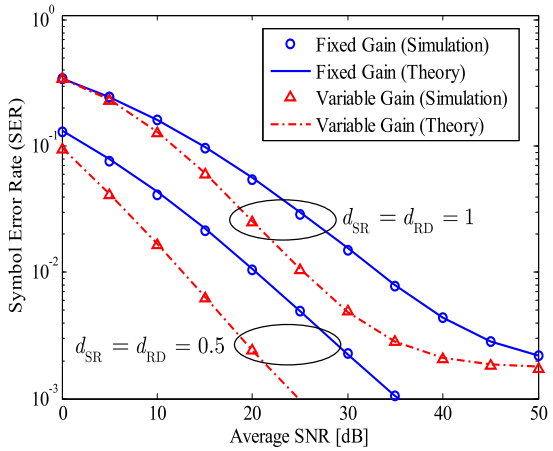

Fig. 4. The SER of the considered FD-V2V communication system using BPSK modulation with $\alpha = 4$, $\tilde{\Omega} = -30$ dB.

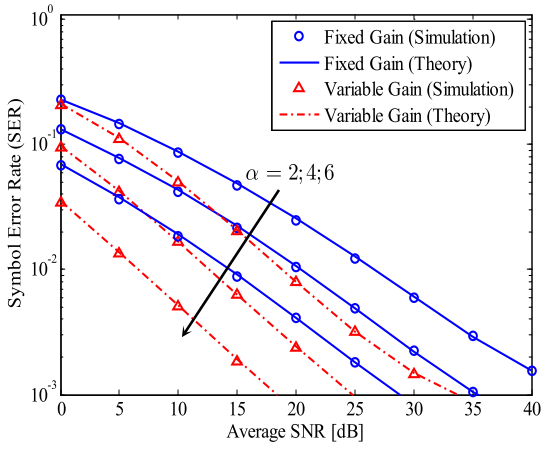

Fig. 5. The impact of path loss exponent on the SER of the considered FD-V2V communication system versus the average SNR for different path loss exponents, $d_{SR} = d_{RD} = 0.5$ and $\tilde{\Omega} = -30$ dB.

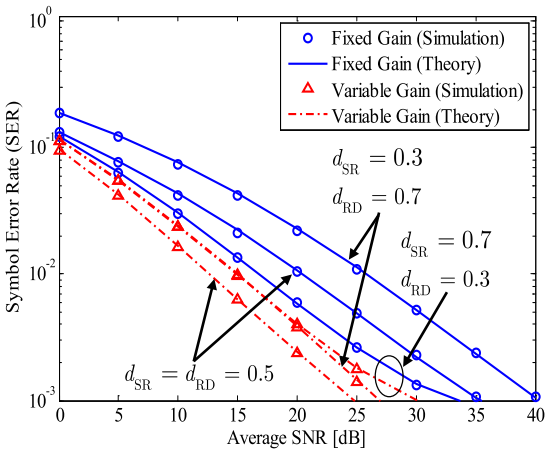

Fig. 6. The SER of the considered FD-V2V communication system versus the average SNR for different settings of the distances among vehicles, $\tilde{\Omega} = -30$ dB.

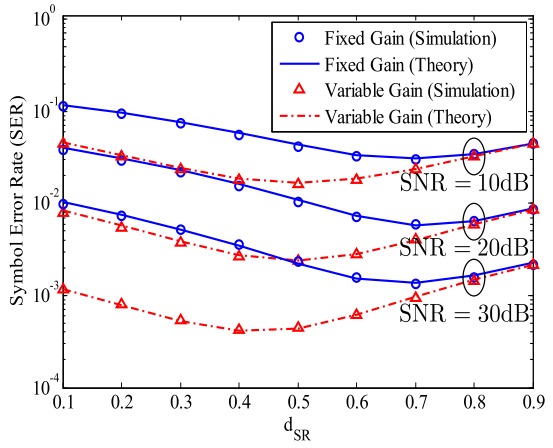

Fig. 7. The SERs of the considered system versus the distance d_{SR} for different average SNRs.

Fig. 4 shows the SER of the considered FD-V2V communication system using BPSK modulation ($a = 1, b = 2$) versus the average SNR with $\alpha = 4$ and $\tilde{\Omega} = -30$ dB. We consider two cases of the distance, i.e. $d_{SR} = d_{RD} = 1$ and $d_{SR} = d_{RD} = 0.5$. Fig. 4 shows that the theory curves which are plotted by using the Theorem 2 are matched with the simulation ones. In the case of $d_{SR} = d_{RD} = 1$, the SER of variable gain relaying goes down slowly and reaches the error floor in high SNR regime while SER of fixed gain relaying continuously goes down. We should notice that both fixed and variable gain relaying have the same error floor when SNR $\to \infty$. Furthermore, as the distance decreases, i.e. $d_{SR} = d_{RD} = 0.5$, the difference between the SERs of fixed and variable gain relaying is increased.

In Fig. 5, we investigate the impact of path loss exponent on the SER of the considered FD-V2V communication system with $d_{SR} = d_{RD} = 0.5$ and $\tilde{\Omega} = -30$ dB. Due to the fact that the distances (d_{SR}, d_{RD}) are smaller than 1, thus larger α results in better SER. As shown in Fig. 5, both SERs in cases of fixed and variable gain relaying increase significantly when $\alpha = 6$ in comparison with those when $\alpha = 2$. At SER $= 10^{-2}$, the differences in the average SNRs of fixed and variable gain relaying when $\alpha = 6$ are approximate 10 dB in comparison with those when $\alpha = 2$. Therefore, when the system operates in the environment which has high path loss exponent, it is necessary to apply various methods such as channel coding, orthogonal frequency division multiplexing (OFDM) to enhance the signal quality.

Fig. 6 shows the SER of the FD-V2V communication system versus the average SNR under the impact of the RSI and the distance between vehicles. We consider $d_{SR} + d_{RD} = 1$, $\alpha = 4$, and $\tilde{\Omega} = -30$ dB. Fig. 6 indicates clearly that the SER of the system significantly depends on d_{SR} and d_{RD}. For the variable gain relaying, the SER is lowest when $d_{SR} = d_{RD} = 0.5$ and when $d_{SR} = 0.7$ and $d_{RD} = 0.3$ for fixed gain relaying. Furthermore, when $d_{SR} = 0.3$ and $d_{RD} = 0.7$, the difference between the SERs of fixed gain relaying and variable gain relaying is the largest in three considered cases. In the case of $d_{SR} = 0.7$ and $d_{RD} = 0.3$, the difference is smallest. Therefore, depending on whether fixed or variable gain relaying is applied, suitable distances between vehicles should be chosen so that better SER can be achieved. On the other hand, when the summation of the distances is a constant, there exist optimal values of d_{SR} and d_{RD} in both fixed and variable gain relaying. Thus, in the next figure, we will investigate this feature in detail.

In Fig. 7, we study the impact of the distance d_{SR} on the SER of the considered FD-V2V communication system. We evaluate the SERs with $d_{SR} + d_{RD} = 1$ for three cases of the SNR i.e. SNR $= 10, 20, 30$ dB. It is obvious that the optimal values of d_{SR} for fixed and variable gain relaying are different. For the fixed gain relaying, the optimal distances are $d_{SR} = 0.7$ and $d_{RD} = 0.3$ for three considered cases of the SNR. For the variable gain relaying, the optimal distances depends on the SNR. When SNR $= 10$, 20 dB, the optimal distances are $d_{SR} = d_{RD} = 0.5$. However, when SNR $= 30$ dB, the optimal distances are $d_{SR} = 0.4$ and $d_{RD} = 0.6$.

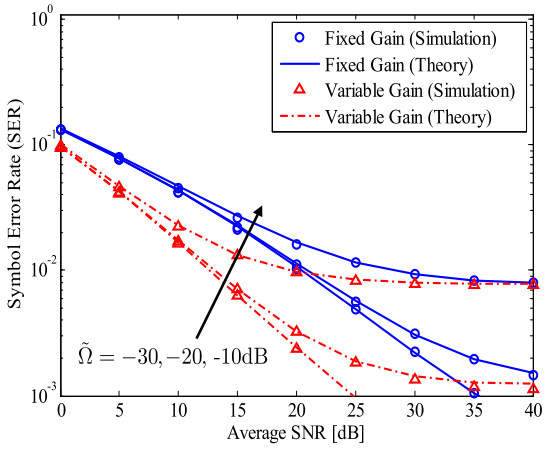

Fig. 8. The impact of RSI on SER of the considered FD-V2V communication system with $d_{SR} = d_{RD} = 0.5, \alpha = 4$.

Finally, Fig. 8 illustrates the impact of the RSI on the SER of the considered FD-V2V communication system with $d_{SR} = d_{RD} = 0.5, \alpha = 4$. This figure represents the importance of SIC capability on the FD system. In the case of small RSI, such as $\tilde{\Omega} = -30$ dB, the SERs continuously go down as SNR increases. However, when the RSI is stronger, such as $\tilde{\Omega} = -20, -10$ dB, the SERs go down slowly and reach the error floor faster. For the variable gain relaying, the SERs reach the error floor at SNR = 30 dB when $\tilde{\Omega} = -20$ dB and at SNR = 20 dB when $\tilde{\Omega} = -10$ dB. We can also see that the SERs of variable gain relaying is lower than those of fixed gain relaying, not only in Fig. 8 but also in other figures.

5. Conclusion

The FD-V2V communication system which combines the FD technique and the V2V communication is a promising system for the future wireless networks. In this paper, we studied the performance of this system where the relay operates in FD mode and uses two cases of AF protocol at the FD relay, i.e. fixed and variable gain relaying. Particularly, we successfully derived the exact closed-form expressions of the OP and SER in these two cases over double Rayleigh fading channels. The impacts of the distance, path loss exponent, and the residual self-interference were also taken into consideration. Based on the derived expressions, we compared the performance of the considered FD-V2V communication system with the performance of this system over Rayleigh fading channels. From the numerical results, some important conclusions can be summarized as follows:

- The performance of the considered FD-V2V communication system degrades stronger than the performance of this system over Rayleigh fading channels for both fixed and variable gain relaying.
- The optimal distances between vehicles for fixed and variable gain relaying are different and closely affect the performance gap between these two cases of AF protocol. From this observed feature, we can choose suitable distances between vehicles in the considered FD-V2V communication system to get the best system performance.

In the near future, we will extend this work by analyzing the scenario where the interference is considered as useful signal for V2V communication systems.

Declaration of Competing Interest

The authors declare that they have no known competing financial interests or personal relationships that could have appeared to influence the work reported in this paper.

Appendix A

This appendix provides the step-by-step derivations, showing how to obtain the OPs in the cases of fixed and variable gain relaying of the considered FD-V2V communication system over double Rayleigh fading channels.

Firstly, we start with the Rayleigh fading channel. The probability density function (PDF) and cumulative distribution function (CDF) of its instantaneous channel gain $\rho = |g|^2$ are respectively given by

$$f_\rho(x) = \frac{1}{\Omega}\exp\left(-\frac{x}{\Omega}\right), \tag{16}$$

$$F_\rho(x) = 1 - \exp\left(-\frac{x}{\Omega}\right), \tag{17}$$

where $\Omega = \mathbb{E}\{\rho\}$.

For the double Rayleigh fading channel in V2V communication, its instantaneous channel gain $|h|^2$ is characterized as the multiplication of two independent variables $|g_1|^2$ and $|g_2|^2$, i.e. $|h|^2 = |g_1|^2|g_2|^2 = \rho_1\rho_2$, where $|g_1|^2$ and $|g_2|^2$ are the instantaneous channel gains of the Rayleigh fading channels. Due to the fact that ρ_1 and ρ_2 are independent variables, we have the CDF of $|h|^2$ as

$$\begin{aligned} F_{|h|^2}(x) &= \Pr(\rho_1\rho_2 \le x) \\ &= \int_0^\infty \Pr\left(\rho_2 \le \frac{x}{\rho_1}\right) f_{\rho_1}(y)dy \\ &= 1 - \frac{1}{\Omega_1}\int_0^\infty \exp\left(-\frac{y}{\Omega_1} - \frac{x}{y\Omega_2}\right)dy \\ &= 1 - \sqrt{\frac{4x}{\Omega_1\Omega_2}}K_1\left(\sqrt{\frac{4x}{\Omega_1\Omega_2}}\right). \end{aligned} \tag{18}$$

Then, we can obtain the PDF of $|h|^2$ as

$$f_{|h|^2}(x) = \frac{2}{\Omega_1\Omega_2}K_0\left(\sqrt{\frac{4x}{\Omega_1\Omega_2}}\right), \tag{19}$$

where $\Omega_1 = \mathbb{E}\{\rho_1\}, \Omega_2 = \mathbb{E}\{\rho_2\}$.

We should note that the PDF and CDF of $|h|^2$ implicitly take into account the effects of scatterers around the transmitter and the receiver which include the fluctuating amplitude and phase of the signals, the Doppler shifts caused by the movement of vehicles [39]. Therefore, as can be seen from (18), the double Rayleigh fading remarkably increases the computation complexity compared with (17) of the Rayleigh fading.

From (10), we have

$$\begin{aligned} P_{\text{out}}^{\text{f}} &= \Pr\{\gamma_{\text{f}} < \gamma_0\} \\ &= \Pr\left\{\frac{(d_{SR}d_{RD})^{-\alpha}P_S P_R XY}{d_{RD}^{-\alpha}P_R Y(\gamma_{RSI}+\sigma^2)+\sigma^2/G_{\text{f}}^2} < \gamma_0\right\}, \end{aligned} \tag{20}$$

$$P_{\text{out}}^{\text{v}} = \Pr\{\gamma_{\text{v}} < \gamma_0\} = \Pr\left\{\frac{(d_{\text{SR}}d_{\text{RD}})^{-\alpha}P_{\text{S}}P_{\text{R}}XY}{d_{\text{RD}}^{-\alpha}P_{\text{R}}Y(\gamma_{\text{RSI}}+\sigma^2)+\sigma^2(d_{\text{SR}}^{-\alpha}P_{\text{S}}X+\gamma_{\text{RSI}}+\sigma^2)} < \gamma_0\right\}, \quad (21)$$

where $X = \rho_1\rho_2$; $Y = \rho_3\rho_4$.

Combining with the PDF and CDF of the instantaneous channel gain of double Rayleigh fading channel given in (18) and (19), we can calculate the $P_{\text{out}}^{\text{f}}$ and $P_{\text{out}}^{\text{v}}$ as follows.

For the $P_{\text{out}}^{\text{f}}$, from (20), we have

$$\begin{aligned}P_{\text{out}}^{\text{f}} &= \Pr\left\{\frac{(d_{\text{SR}}d_{\text{RD}})^{-\alpha}P_{\text{S}}P_{\text{R}}XY}{d_{\text{RD}}^{-\alpha}P_{\text{R}}Y(\gamma_{\text{RSI}}+\sigma^2)+\sigma^2/G_{\text{f}}^2} < \gamma_0\right\}\\ &= \Pr\left\{X < \frac{\sigma^2\gamma_0}{G_{\text{f}}^2(d_{\text{SR}}d_{\text{RD}})^{-\alpha}P_{\text{S}}P_{\text{R}}Y} + \frac{(\gamma_{\text{RSI}}+\sigma^2)\gamma_0}{d_{\text{SR}}^{-\alpha}P_{\text{S}}}\right\}\\ &= 1-\int_0^{\infty}\left[1-F_X\left(\frac{\sigma^2\gamma_0}{G_{\text{f}}^2(d_{\text{SR}}d_{\text{RD}})^{-\alpha}P_{\text{S}}P_{\text{R}}\xi}\right.\right.\\ &\quad\left.\left.+\frac{(\gamma_{\text{RSI}}+\sigma^2)\gamma_0}{d_{\text{SR}}^{-\alpha}P_{\text{S}}}\right)\right]f_Y(\xi)d\xi. \quad (22)\end{aligned}$$

Since X and Y are the instantaneous channel gains of double Rayleigh fading channels, the PDF and CDF of X and Y are given in (18) and (19), respectively. Therefore, the $P_{\text{out}}^{\text{f}}$ is calculated as

$$\begin{aligned}P_{\text{out}}^{\text{f}} &= 1-\int_0^{\infty}\sqrt{\frac{4\sigma^2\gamma_0}{\Omega_1\Omega_2G_{\text{f}}^2(d_{\text{SR}}d_{\text{RD}})^{-\alpha}P_{\text{S}}P_{\text{R}}\xi}+\frac{4(\gamma_{\text{RSI}}+\sigma^2)\gamma_0}{\Omega_1\Omega_2d_{\text{SR}}^{-\alpha}P_{\text{S}}}}\\ &\quad\times K_1\left(\sqrt{\frac{4\sigma^2\gamma_0}{\Omega_1\Omega_2G_{\text{f}}^2(d_{\text{SR}}d_{\text{RD}})^{-\alpha}P_{\text{S}}P_{\text{R}}\xi}+\frac{4(\gamma_{\text{RSI}}+\sigma^2)\gamma_0}{\Omega_1\Omega_2d_{\text{SR}}^{-\alpha}P_{\text{S}}}}\right)\\ &\quad\times\frac{2}{\Omega_3\Omega_4}K_0\left(\sqrt{\frac{4\xi}{\Omega_3\Omega_4}}\right)d\xi\\ &= 1-C_{\text{f}}\int_0^{\infty}\sqrt{\frac{A_{\text{f}}\gamma_0}{\xi}+B_{\text{f}}\gamma_0}K_1\left(\sqrt{\frac{A_{\text{f}}\gamma_0}{\xi}+B_{\text{f}}\gamma_0}\right)\\ &\quad\times K_0(\sqrt{2C_{\text{f}}\xi})d\xi. \quad (23)\end{aligned}$$

Next, by setting $\upsilon = e^{-\xi}$, (23) can be rewritten as

$$\begin{aligned}P_{\text{out}}^{\text{f}} &= 1-C_{\text{f}}\int_0^{1}\sqrt{\frac{A_{\text{f}}\gamma_0}{-\ln\upsilon}+B_{\text{f}}\gamma_0}K_1\left(\sqrt{\frac{A_{\text{f}}\gamma_0}{-\ln\upsilon}+B_{\text{f}}\gamma_0}\right)\\ &\quad\times K_0(\sqrt{-2C_{\text{f}}\ln\upsilon})\frac{d\upsilon}{\upsilon}. \quad (24)\end{aligned}$$

Applying the Gaussian-Chebyshev quadrature method [40], (24) becomes (11).

For the $P_{\text{out}}^{\text{v}}$, from (21), we have

$$\begin{aligned}P_{\text{out}}^{\text{v}} &= \Pr\left\{\frac{(d_{\text{SR}}d_{\text{RD}})^{-\alpha}P_{\text{S}}P_{\text{R}}XY}{d_{\text{RD}}^{-\alpha}P_{\text{R}}Y(\gamma_{\text{RSI}}+\sigma^2)+\sigma^2(d_{\text{SR}}^{-\alpha}P_{\text{S}}X+\gamma_{\text{RSI}}+\sigma^2)} < \gamma_0\right\}\\ &= \Pr\left\{d_{\text{SR}}^{-\alpha}XP_{\text{S}}\left(d_{\text{RD}}^{-\alpha}P_{\text{R}}Y-\sigma^2\gamma_0\right)\right.\\ &\quad\left.< d_{\text{RD}}^{-\alpha}P_{\text{R}}Y\left(\gamma_{\text{RSI}}+\sigma^2\right)\gamma_0+\left(\gamma_{\text{RSI}}+\sigma^2\right)\sigma^2\gamma_0\right\}. \quad (25)\end{aligned}$$

Then, by setting $Y = Z + \frac{\sigma^2\gamma_0}{d_{\text{RD}}^{-\alpha}P_{\text{R}}}$, (25) becomes

$$P_{\text{out}}^{\text{v}} = \Pr\left\{(d_{\text{SR}}d_{\text{RD}})^{-\alpha}P_{\text{S}}P_{\text{R}}XZ < d_{\text{RD}}^{-\alpha}P_{\text{R}}\left(Z+\frac{\sigma^2\gamma_0}{d_{\text{RD}}^{-\alpha}P_{\text{R}}}\right)\times\left(\gamma_{\text{RSI}}+\sigma^2\right)\gamma_0+\left(\gamma_{\text{RSI}}+\sigma^2\right)\sigma^2\gamma_0\right\}. \quad (26)$$

From (26), we can calculate the $P_{\text{out}}^{\text{v}}$ by using the same method as for $P_{\text{out}}^{\text{f}}$, i.e.,

$$\begin{aligned}P_{\text{out}}^{\text{v}} &= 1-\int_0^{\infty}\left[1-F_X\left(\frac{(\gamma_{\text{RSI}}+\sigma^2)\sigma^2(\gamma_0+\gamma_0^2)}{(d_{\text{SR}}d_{\text{RD}})^{-\alpha}P_{\text{S}}P_{\text{R}}\xi}\right.\right.\\ &\quad\left.\left.+\frac{(\gamma_{\text{RSI}}+\sigma^2)\gamma_0}{d_{\text{SR}}^{-\alpha}P_{\text{S}}}\right)\right]f_Z\left(\xi+\frac{\sigma^2\gamma_0}{d_{\text{RD}}^{-\alpha}P_{\text{R}}}\right)d\xi\\ &= 1-\int_0^{\infty}\sqrt{\frac{(4\gamma_{\text{RSI}}+\sigma^2)\sigma^2(\gamma_0+\gamma_0^2)}{\Omega_1\Omega_2(d_{\text{SR}}d_{\text{RD}})^{-\alpha}P_{\text{S}}P_{\text{R}}\xi}+\frac{4(\gamma_{\text{RSI}}+\sigma^2)\gamma_0}{\Omega_1\Omega_2d_{\text{SR}}^{-\alpha}P_{\text{S}}}}\\ &\quad\times K_1\left(\sqrt{\frac{(4\gamma_{\text{RSI}}+\sigma^2)\sigma^2(\gamma_0+\gamma_0^2)}{\Omega_1\Omega_2(d_{\text{SR}}d_{\text{RD}})^{-\alpha}P_{\text{S}}P_{\text{R}}\xi}+\frac{4(\gamma_{\text{RSI}}+\sigma^2)\gamma_0}{\Omega_1\Omega_2d_{\text{SR}}^{-\alpha}P_{\text{S}}}}\right)\\ &\quad\times\frac{2}{\Omega_3\Omega_4}K_0\left(\sqrt{\frac{4(\xi+\frac{\sigma^2\gamma_0}{d_{\text{RD}}^{-\alpha}P_{\text{R}}})}{\Omega_3\Omega_4}}\right)d\xi\\ &= 1-C_{\text{v}}\int_0^{\infty}\sqrt{\frac{A_{\text{v}}(\gamma_0+\gamma_0^2)}{\xi}+B_{\text{v}}\gamma_0}\\ &\quad\times K_1\left(\sqrt{\frac{A_{\text{v}}(\gamma_0+\gamma_0^2)}{\xi}+B_{\text{v}}\gamma_0}\right)\\ &\quad\times K_0(\sqrt{2C_{\text{v}}\xi+D_{\text{v}}\gamma_0})d\xi. \quad (27)\end{aligned}$$

We denote $\upsilon = e^{-\xi}$. Then, (27) can be rewritten as

$$\begin{aligned}P_{\text{out}}^{\text{v}} &= 1-C_{\text{v}}\int_0^{1}\sqrt{\frac{A_{\text{v}}(\gamma_0+\gamma_0^2)}{-\ln\upsilon}+B_{\text{v}}\gamma_0}\\ &\quad\times K_1\left(\sqrt{\frac{A_{\text{v}}(\gamma_0+\gamma_0^2)}{-\ln\upsilon}+B_{\text{v}}\gamma_0}\right)\\ &\quad\times K_0\left(\sqrt{2C_{\text{v}}(-\ln\upsilon)+D_{\text{v}}\gamma_0}\right)\frac{d\upsilon}{\upsilon}. \quad (28)\end{aligned}$$

Similarly, using the Gaussian-Chebyshev quadrature method [40], (28) becomes (12). The proof of Appendix A is complete.

Appendix B

This appendix presents detailed derivations to obtain the SER_{f} and SER_{v} of the considered FD-V2V communication system.

From (13), after some mathematical transforms, the SER is given by

$$\text{SER} = \frac{a\sqrt{b}}{2\sqrt{2\pi}}\int_0^{\infty}\frac{e^{-bx/2}}{\sqrt{x}}F(x)dx. \quad (29)$$

Then, we substitute $F(x)$ in (29) by $P_{\text{out}}^{\text{f}}$ in (11) to obtain SER_{f} and by $P_{\text{out}}^{\text{v}}$ in (12) to obtain SER_{v}. More specifically, SER_{f} is computed as

$$\mathrm{SER_f} = \frac{a\sqrt{b}}{2\sqrt{2\pi}}\Bigg[\int_0^\infty \frac{e^{-bx/2}}{\sqrt{x}}dx - \int_0^\infty \frac{e^{-bx/2}}{\sqrt{x}}\frac{\pi C_\mathrm{f}}{2M}\sum_{m=1}^{M}\frac{\sqrt{1-\phi_m^2}}{z} \times \sqrt{\frac{A_\mathrm{f}x}{-\ln z}+B_\mathrm{f}x}K_0(\sqrt{-2C_\mathrm{f}\ln z})K_1\left(\sqrt{\frac{A_\mathrm{f}x}{-\ln z}+B_\mathrm{f}x}\right)dx\Bigg]$$
$$= \frac{a\sqrt{b}}{2\sqrt{2\pi}}\Bigg[\int_0^\infty \frac{e^{-bx/2}}{\sqrt{x}}dx - \frac{\pi C_\mathrm{f}}{2M}\sum_{m=1}^{M}\frac{\sqrt{1-\phi_m^2}}{z}\sqrt{\frac{A_\mathrm{f}}{-\ln z}+B_\mathrm{f}} \times K_0(\sqrt{-2C_\mathrm{f}\ln z})\int_0^\infty e^{-bx/2}K_1\left(\sqrt{\frac{A_\mathrm{f}x}{-\ln z}+B_\mathrm{f}x}\right)dx\Bigg]. \quad (30)$$

To derive the closed-form expression of the first integral in (30), we use [37, Eq.3.361.2] to get

$$\int_0^\infty \frac{e^{-bx/2}}{\sqrt{x}}dx = \sqrt{\frac{2\pi}{b}}. \quad (31)$$

For the second integral in (30), we apply [37, Eq. 6.614.4] to have

$$\int_0^\infty e^{-bx/2}K_1\left(\sqrt{\frac{A_\mathrm{f}x}{-\ln z}+B_\mathrm{f}x}\right)dx = \exp\left(\frac{1}{4b}\left(\frac{A_\mathrm{f}}{-\ln z}+B_\mathrm{f}\right)\right)\frac{\Gamma(\frac{3}{2})\Gamma(\frac{1}{2})}{\sqrt{\frac{b}{2}(\frac{A_\mathrm{f}}{-\ln z}+B_\mathrm{f})}} \times W_{-\frac{1}{2},\frac{1}{2}}\left(\frac{1}{2b}\left(\frac{A_\mathrm{f}}{-\ln z}+B_\mathrm{f}\right)\right). \quad (32)$$

Then, we substitute (31) and (32) into (30) to obtain the $\mathrm{SER_f}$ as in (14).

Similar to the $\mathrm{SER_f}$, the $\mathrm{SER_v}$ is calculated as

$$\mathrm{SER_v} = \frac{a\sqrt{b}}{2\sqrt{2\pi}}\Bigg[\int_0^\infty \frac{e^{-bx/2}}{\sqrt{x}}dx - \int_0^\infty \frac{e^{-bx/2}}{\sqrt{x}}\frac{\pi C_\mathrm{v}}{2M}\sum_{m=1}^{M}\frac{\sqrt{1-\phi_m^2}}{z} \times \sqrt{\frac{A_\mathrm{v}(x^2+x)}{-\ln z}+B_\mathrm{v}x}K_0(\sqrt{-2C_\mathrm{v}\ln z+D_\mathrm{v}x}) \times K_1\left(\sqrt{\frac{A_\mathrm{v}(x^2+x)}{-\ln z}+B_\mathrm{v}x}\right)dx\Bigg]$$
$$= \frac{a\sqrt{b}}{2\sqrt{2\pi}}\Bigg[\int_0^\infty \frac{e^{-bx/2}}{\sqrt{x}}dx - \frac{\pi C_\mathrm{v}}{2M}\sum_{m=1}^{M}\frac{\sqrt{1-\phi_m^2}}{z}\int_0^\infty \times e^{-bx/2}\sqrt{\frac{A_\mathrm{v}(x+1)}{-\ln z}+B_\mathrm{v}}K_0(\sqrt{-2C_\mathrm{v}\ln z+D_\mathrm{v}x}) \times K_1\left(\sqrt{\frac{A_\mathrm{v}(x^2+x)}{-\ln z}+B_\mathrm{v}x}\right)dx\Bigg]. \quad (33)$$

To derive the closed-form expression of the second integral in (33), we set $\chi = e^{-bx/2}$. Thus, $x = -\frac{2}{b}\ln\chi$, and the second integral in (33) can be rewritten as

$$\int_0^\infty e^{-bx/2}\sqrt{\frac{A_\mathrm{v}(x+1)}{-\ln z}+B_\mathrm{v}}K_0(\sqrt{-2C_\mathrm{v}\ln z+D_\mathrm{v}x}) \times K_1\left(\sqrt{\frac{A_\mathrm{v}(x^2+x)}{-\ln z}+B_\mathrm{v}x}\right)dx$$
$$= \frac{2}{b}\int_0^1 \sqrt{\frac{A_\mathrm{v}(b-2\ln\chi)}{-b\ln z}+B_\mathrm{v}}K_0\left(\sqrt{-2C_\mathrm{v}\ln z-\frac{2D_\mathrm{v}\ln\chi}{b}}\right) \times K_1\left(\sqrt{-\frac{2}{b}\left[\frac{A_\mathrm{v}(b-2\ln\chi)}{-b\ln z}+B_\mathrm{v}\right]\ln\chi}\right)d\chi. \quad (34)$$

Then, we use the Gaussian-Chebyshev quadrature method in [40] to derive the closed-form expression of the integral in (34). After that, we combine this expression with (31) to obtain the $\mathrm{SER_v}$ as in (15). The proof is complete.

References

[1] F.-L. Luo, C. Zhang, Signal Processing for 5G: Algorithms and Implementations, John Wiley & Sons, 2016.

[2] Q.C. Li, H. Niu, A.T. Papathanassiou, G. Wu, 5g network capacity: key elements and technologies, IEEE Veh. Technol. Mag. 9 (1) (2014) 71–78.

[3] Y. Alsaba, C.Y. Leow, S.K.A. Rahim, Full-duplex cooperative non-orthogonal multiple access with beamforming and energy harvesting, in: IEEE Access, vol. 6, 2018, pp. 19 726–19 738.

[4] D. Bharadia, E. McMilin, S. Katti, Full duplex radios, in: ACM SIGCOMM Computer Communication Review, vol. 43, issue 4, ACM, 2013, pp. 375–386.

[5] A. Sabharwal, P. Schniter, D. Guo, D.W. Bliss, S. Rangarajan, R. Wichman, In-band full-duplex wireless: challenges and opportunities, IEEE J. Sel. Areas Commun. 32 (9) (2014) 1637–1652.

[6] X. Li, C. Tepedelenlioglu, H. Senol, Channel estimation for residual self-interference in full duplex amplify-and-forward two-way relays, IEEE Trans. Wirel. Commun. 99 (2017) 1.

[7] E. Antonio-Rodríguez, R. López-Valcarce, T. Riihonen, S. Werner, R. Wichman, Adaptive self-interference cancellation in wideband full-duplex decode-and-forward MIMO relays, in: 2013 IEEE 14th Workshop on Signal Processing Advances in Wireless Communications, SPAWC, IEEE, 2013, pp. 370–374.

[8] O. Abbasi, A. Ebrahimi, Cooperative NOMA with full-duplex amplify-and-forward relaying, Transp. Emerg. Telecommun. Technol. 29 (7) (2018) e3421.

[9] B.C. Nguyen, X.N. Tran, D.T. Tran, Performance analysis of in-band full-duplex amplify-and-forward relay system with direct link, in: 2018 2nd International Conference on Recent Advances in Signal Processing, Telecommunications & Computing, SigTelCom, IEEE, 2018, pp. 192–197.

[10] B.C. Nguyen, T.M. Hoang, P.T. Tran, Performance analysis of full-duplex decode-and-forward relay system with energy harvesting over Nakagami-m fading channels, AEÜ, Int. J. Electron. Commun. 98 (2019) 114–122.

[11] T.M. Hoang, V. Van Son, N.C. Dinh, P.T. Hiep, Optimizing duration of energy harvesting for downlink NOMA full-duplex over Nakagami-m fading channel, AEÜ, Int. J. Electron. Commun. (2018).

[12] A. Zanella, A. Bazzi, B.M. Masini, Relay selection analysis for an opportunistic two-hop multi-user system in a Poisson field of nodes, IEEE Trans. Wirel. Commun. 16 (2) (2016) 1281–1293.

[13] C. La Palombara, V. Tralli, B.M. Masini, A. Conti, Relay-assisted diversity communications, IEEE Trans. Veh. Technol. 62 (1) (2012) 415–421.

[14] X.N. Tran, B.C. Nguyen, D.T. Tran, Outage probability of two-way full-duplex relay system with hardware impairments, in: 2019 3rd International Conference on Recent Advances in Signal Processing, Telecommunications & Computing, SigTelCom, IEEE, 2019, pp. 135–139.

[15] G.J. Gonzalez, F.H. Gregorio, J.E. Cousseau, T. Riihonen, R. Wichman, Full-duplex amplify-and-forward relays with optimized transmission power under imperfect transceiver electronics, EURASIP J. Wirel. Commun. Netw. 2017 (76) (2017) 1–12.

[16] G. Naik, B. Choudhury, et al., IEEE 802.11 bd & 5g nr v2x: evolution of radio access technologies for v2x communications, arXiv preprint, arXiv:1903.08391, 2019.

[17] A. Nabil, K. Kaur, C. Dietrich, V. Marojevic, Performance analysis of sensing-based semi-persistent scheduling in c-v2x networks, in: 2018 IEEE 88th Vehicular Technology Conference, VTC-Fall, IEEE, 2019, pp. 1–5.

[18] S. Biswas, R. Tatchikou, F. Dion, Vehicle-to-vehicle wireless communication protocols for enhancing highway traffic safety, IEEE Commun. Mag. 44 (1) (2006) 74–82.

[19] C. Campolo, A. Molinaro, A.O. Berthet, A. Vinel, Full-duplex radios for vehicular communications, IEEE Commun. Mag. 55 (6) (2017) 182–189.

[20] Y. Ai, M. Cheffena, A. Mathur, H. Lei, On physical layer security of double Rayleigh fading channels for vehicular communications, IEEE Wirel. Commun. Lett. 7 (6) (2018) 1038–1041.

[21] A.S. Akki, F. Haber, A statistical model of mobile-to-mobile land communication channel, IEEE Trans. Veh. Technol. 35 (1) (1986) 2–7.

[22] I.Z. Kovacs, Radio Channel Characterisation for Private Mobile Radio Systems-Mobile-to-Mobile Radio Link Investigations, Ph.D. dissertation, Aalborg Universitet, 2002.

[23] V. Erceg, S.J. Fortune, J. Ling, A. Rustako, R.A. Valenzuela, Comparisons of a computer-based propagation prediction tool with experimental data collected in urban microcellular environments, IEEE J. Sel. Areas Commun. 15 (4) (1997) 677–684.
[24] D. Chizhik, J. Ling, P.W. Wolniansky, R.A. Valenzuela, N. Costa, K. Huber, Multiple-input-multiple-output measurements and modeling in Manhattan, IEEE J. Sel. Areas Commun. 21 (3) (April 2003) 321–331.
[25] J. Wu, C. Xiao, Performance analysis of wireless systems with doubly selective Rayleigh fading, IEEE Trans. Veh. Technol. 56 (2) (2007) 721–730.
[26] M. Seyfi, S. Muhaidat, J. Liang, M. Uysal, Relay selection in dual-hop vehicular networks, IEEE Signal Process. Lett. 18 (2) (2011) 134–137.
[27] Y. Chen, L. Wang, Y. Ai, B. Jiao, L. Hanzo, Performance analysis of NOMA-SM in vehicle-to-vehicle massive MIMO channels, IEEE J. Sel. Areas Commun. 35 (12) (2017) 2653–2666.
[28] T.T. Duy, G.C. Alexandropoulos, V.T. Tung, V.N. Son, T.Q. Duong, Outage performance of cognitive cooperative networks with relay selection over double-Rayleigh fading channels, IET Commun. 10 (1) (2016) 57–64.
[29] H. Lei, I.S. Ansari, G. Pan, B. Alomair, M.-S. Alouini, Secrecy capacity analysis over α-μ fading channels, IEEE Commun. Lett. 21 (6) (2017) 1445–1448.
[30] A. Bazzi, C. Campolo, B.M. Masini, A. Molinaro, A. Zanella, A.O. Berthet, Enhancing cooperative driving in IEEE 802.11 vehicular networks through full-duplex radios, IEEE Trans. Wirel. Commun. 17 (4) (2018) 2402–2416.
[31] C.-X. Mao, S. Gao, Y. Wang, Dual-band full-duplex Tx/Rx antennas for vehicular communications, IEEE Trans. Veh. Technol. 67 (5) (2018) 4059–4070.
[32] M. Yang, S.-W. Jeon, D.K. Kim, Interference management for in-band full-duplex vehicular access networks, IEEE Trans. Veh. Technol. 67 (2) (2018) 1820–1824.
[33] S. Hong, J. Brand, J.I. Choi, M. Jain, J. Mehlman, S. Katti, P. Levis, Applications of self-interference cancellation in 5G and beyond, IEEE Commun. Mag. 52 (2) (Feb. 2014) 114–121.
[34] F. Jameel, S. Wyne, M.A. Javed, S. Zeadally, Interference-aided vehicular networks: future research opportunities and challenges, IEEE Commun. Mag. 56 (10) (2018) 36–42.
[35] K. Yang, H. Cui, L. Song, Y. Li, Efficient full-duplex relaying with joint antenna-relay selection and self-interference suppression, IEEE Trans. Wirel. Commun. 14 (7) (Jul. 2015) 3991–4005.
[36] A. Goldsmith, Wireless Communications, Cambridge University Press, 2005.
[37] A. Jeffrey, D. Zwillinger, Table of Integrals, Series, and Products, Academic Press, 2007.
[38] C. Li, Z. Chen, Y. Wang, Y. Yao, B. Xia, Outage analysis of the full-duplex decode-and-forward two-way relay system, IEEE Trans. Veh. Technol. 66 (5) (May 2017) 4073–4086.
[39] I.Z. Kovacs, P.C.F. Eggers, K. Olesen, L.G. Petersen, Investigations of outdoor-to-indoor mobile-to-mobile radio communication channels, in: Proceedings IEEE 56th Vehicular Technology Conference, vol. 1, IEEE, 2002, pp. 430–434.
[40] M. Abramowitz, I.A. Stegun, Handbook of Mathematical Functions with Formulas, Graphs, and Mathematical Tables, vol. 9, Dover, New York, 1972.